Vietnam Journal of Earth Sciences, 44(2), 273-285, https://doi.org/10.15625/2615-9783/16998

Vietnam Academy of Science and Technology
Vietnam Journal of Earth Sciences
http://www.vjs.ac.vn/index.php/jse

Removal of methylene blue from aqueous solution by biochar derived from rice husk

Huyen Thuong Bui[1], Phuong Thu Le[1*], Thu Phuong Nguyen[2*], Duy Ngoc Le[1], Dieu Linh Vo[1], Le Anh Pham[1], Luong Lam Nguyen[1], Thi Hue Nguyen[3,4], Tuan Vinh Le[3,4], Mai Huong[1], Thi Mai Thanh Dinh[1,2], Marine Herrmann[1,5], Sylvain Ouillon[1,5], Thi Thuy Duong[3,4], Thi Phuong Quynh Le[6]

[1]*University of Science and Technology of Hanoi, VAST, Hanoi, Vietnam*
[2]*Institute for Tropical Technology, VAST, Hanoi, Vietnam*
[3]*Institute of Environmental Technology, VAST, Hanoi, Vietnam*
[4]*Graduate University of Science and Technology, VAST, Hanoi, Vietnam*
[5]*UMR 5566 LEGOS, Université de Toulouse, IRD, CNES, CNRS, UPS, 14 avenue Edouard Belin, 31400 Toulouse, France*
[6]*Institute of Natural Products Chemistry, VAST, Hanoi, Vietnam*

Received 14 October 2021; Received in revised form 28 December 2021; Accepted 15 March 2022

ABSTRACT

In this research, rice husk-derived biochar (BC) was evaluated to determine the suitable conditions for the methylene blue (MB) solution adsorption. The characterization of BC was identified by the methods of FT-IR, Raman, and point of zero charges (PZC). The adsorption studies were carried out with BC at different activation conditions (raw BC, HNO_3 25% for 4 hours, NaOH 25% for 4 hours, H_2O at 90°C for 2 hours and 4 hours, HNO_3 25% at 90°C for 2 hours and 4 hours). The activated material then went through an adsorption assessment. Activated BC with NaOH 25% showed its preeminence compared to the other six conditions when reaching the maximum efficiency after the first hour of adsorption. The investigation revealed that the adsorption capacity of the material depends on the activation methods, including pH, activation agent, temperature, and time. The adsorption of BC was consistent with the pseudo-first-order kinetic model and the Langmuir isotherm model, with high correlation coefficients (R^2: 0.9838 and 0.9975, respectively). Therefore, it can be concluded that the use of rice husk is feasible for the removal of MB from aqueous solutions.

Keywords: Biochar, Methylene blue, adsorption, rice husk.

1. Introduction

Methylene blue ($C_{16}H_{18}ClN_3S$, MB), a cationic dye is being used extensively in chemical indicators and dyes. It is originated from various dyeing processes of the textile industry, which is one of the largest industries in the world but also a serious threat to the environment. The textile industry raises concerns about the discharged wastewater from the dyeing processes (Desore and Narula, 2018), leaving negative impacts on ecosystems and human health (Manzoor and Sharma, 2020). Several properties of dye

*Corresponding author, Email: le-phuong.thu@usth.edu.vn

wastewater, including high discharge, chromaticity, organic matter content, and low biodegradability, negatively impact the health of water bodies and the photosynthesis of microorganisms in the aquatic environment (Kuang et al., 2020). For a long time, scientists have made countless efforts towards the removal of dyes from contaminated water sources (Bisschops and Spanjers, 2003; Lin and Peng, 1994; Paździor et al., 2019). Many conventional methods have been applied to treat textile wastewater (Holkar et al., 2016; Sarayu and Sandhya, 2012), including electrochemical (Sala and Gutiérrez-Bouzán, 2012), photocatalysis (Al-Mamun et al., 2019), biological (Shoukat et al., 2019), or using membranes methods (Laqbaqbi et al., 2019), etc. Within different methods used for textile wastewater treatment, adsorption showed its advantages over other technologies (Siddique et al., 2017) by its high performance, low cost, and ability to remove a wide range of dyes.

With adsorption, the priority is to search for efficient adsorbents matching different wastewater characteristics and conditions. Along with improving the performance of the materials, reducing production expenses must also be a focus. Hence, utilizing agricultural by-products as adsorbents has intrigued the interest of numerous researchers. Biochar (BC) from sugar cane bagasse (Raymundo et al., 2010), sunflower seed hull (Hameed, 2008), palm kernel shell (Kyi et al., 2020), pecan nutshell (Zazycki et al., 2018), coir pith, rice husk (Rubeena et al., 2018), and many more, has proven to be effective in treating textile wastewater.

Taking advantage of Vietnam's agricultural solid background with an abundant supply of agricultural by-products, this study selected BC from rice husks as the adsorbent in the use of removing dye ions from aqueous solutions.

The common BC is not widely used to adsorb and remove pollutants due to its low adsorption capacity, which is caused by a small specific surface area, poor adsorption selection performance, and limitations in the surface functional groups. The surface of activated carbon must be modified in many circumstances to improve its affinity with target pollutants, raise its adsorption capacity, and enhance the removal impact of pollutants in many forms of industrial effluent.

Physical and chemical approaches are all utilized to change BC, and they are all proven to be effective. Various chemical reagents have been known to activate BC, namely $ZnCl_2$ (Ahiduzzaman and Sadrul Islam, 2016), KOH (Wang et al., 2018), NaOH (Acemioğlu, 2019), (Lin et al., 2013), H_3PO_4, HNO_3 (Zhao et al., 2017), etc. According to Dargo et al. (2014), rice husk activated with H_2SO_4 at pH 8-10 showed a removal efficiency yield of methylene blue up to 99%.

In this research, our goal is to determine the impacts of different activation conditions on the capacity of BC adsorption and conduct an isotherm and kinetics analysis of BC adsorption on a cationic dye, methylene blue.

2. Materials and method

2.1. Materials

2.1.1. Chemicals

Methylene blue trihydrate (MB, $C_{16}H_{18}ClN_3S.3H_2O$, ≥ 98.5%) was purchased from Xilong Chemical Co., Ltd. (China). Sodium hydroxide (NaOH, ≥ 99.5%) was from Merck (Germany). Hydrochloric acid (HCl, 35.0-37.0%) and nitric acid (HNO_3, 65%) were obtained from Daejung chemicals and metals (Korea).

2.1.2. Preparation of biochar

The rice husk, received from a local farm, was sieved to collect husk with a diameter of 5 mm. Then, the material was rinsed three times with tap water and twice with distilled water. The clean husk was dried in an oven at 105°C for 5 hours. The pyrolysis of the

material took place in a stainless steel pot with a closed lid. The rice husk was fully covered with a layer of commercial charcoal, this was to prevent the rice husk BC from turning into ash and maintain its original husk shape. The pyrolysis was carried out under a heating program in a Nabertherm furnace (Germany), which raised the temperature to 600°C with a heating rate of 5°C.min^{-1} for a period of 2 hours (Le et al., 2021).

2.1.3. Activation of biochar

To access the effect of activation conditions on the adsorption of MB, six different conditions were conducted, including two conditions at room temperature: HNO_3 25% for 4 hours, NaOH 25% for 4 hours and four conditions at high temperature (T): H_2O at 90°C for 2 hours and 4 hours, HNO_3 25% at 90°C for 2 hours and 4 hours.

For the BC activation at room temperature, BC was activated for 4 hours by HNO_3 25% and by NaOH 25% with the following procedure: In a 500 mL Duran bottle, 18 g of BC and 300 mL of chemical solution were prepared. The bottle was then placed in an IKA KS4000i incubator shaker at 250 rpm for 4 hours at room temperature.

For the BC activation at high temperature, BC was activated by H_2O at 90°C for 2 hours and 4 hours, respectively, and at the same conditions for BC activation with HNO_3 25%. In a round bottom-flask, 18 g of BC and 300 mL of chemical solution were added, then installed into a Soxhlet system with the temperature raised to 90°C for 2 hours or 4 hours. The materials were cooled down for 15 minutes.

All the activated BCs were filtered, washed with Mili-Q water to neutrality, dried in an oven at 105°C for 24 hours, and finally kept in sealed brown bottles.

2.2. Adsorption capacity

Methylene blue trihydrate ($C_{16}H_{18}ClN_3S.3H_2O$) is a cationic dye that can dissociate into positively charged ions in an aqueous solution. To evaluate the MB adsorption capacity by activated BC, 5 g.L^{-1} of BC and 10 mg.L^{-1} of MB solution, precisely at pH = 12 and neutral pH, were chosen.

2.3. Characterization of modified biochar

Many methods were performed to examine the characterization of activated BC. An FTIR spectrometer (Thermo Scientific iS50) was used to identify the functional groups of the BCs with a wavenumber variation from 400 cm^{-1} to 4000 cm^{-1} and the resolution factor at 4 cm^{-1}. A Raman spectrometer (NRS-5100, JASCO Corporation) determined the material's molecules, chemical bonding, and intramolecular bonds. As for the pHpzc, NaCl was added to deionized water to prepare solutions with the concentration of 10^{-2} M and 5×10^{-2} M, then HCl and NaOH were used to customize the pH of the NaCl solution to 2, 4, 6, 8, 10 and 12. In an incubator shaker, bottles of 70 mL adjusted solutions with 0.35 g of BC were shaken for 24 hours. The pH values of the solutions were then collected to make the pH diagrams.

2.4. The study of adsorption kinetics and isotherms

To better understand the mechanism during the adsorption process, the adsorption experiments of BC were conducted with the MB concentration from 10 mg.L^{-1} to 50 mg.L^{-1} with 5 g.L^{-1} of BC. The initial pH of the solution was selected based on the optimal results from the previous experiment. In this study, three kinetic models were evaluated, precisely pseudo first-order (Lagergreen and Svenska, 1907), pseudo second-order (Ho and McKay, 1999), and intraparticle diffusion (Weber and Morris, 1963; Qiu et al., 2009).

The adsorbed capacity of MB (q_t) (mg.g^{-1}) was calculated with the following formula (Robati, 2013):

$$q_t = \frac{(C_0 - C_t) \times V}{W}$$

Where C_0 and C_t (mg.L^{-1}) are the concentrations of the dye at t = 0 and at time t, V is the solution volume (L) and W is the weight of BC (g). The reaction rate equations according to the kinetic models are presented in Table 1.

Table 1. Kinetic model and equations

Kinetic model	Linear equation	Linear graphs	Constant
Pseudo first-order	$\ln(q_e - q_t) = \ln q_e - k_1 t$	$\ln(q_e - q_t)\ vs\ t$	$k_1\ and\ q_e$
Pseudo second-order	$\frac{t}{q_t} = \frac{1}{k_2 {q_e}^2} + \frac{1}{q_e} \times t$	$\frac{t}{q_t}\ vs\ t$	$k_2\ and\ q_e$
Intraparticle diffusion	$q_t = k_{ip} \times t^{1/2} + C_i$	$q_t\ vs\ t^{1/2}$	k_{ip}

In addition, two isotherm models were also under evaluation by Langmuir (1916) and Freundlich (1906).

$$q_e = \frac{(C_0 - C_e) \times V}{W}$$

Here, C_0 and C_e (mg.L^{-1}) are the concentrations of the dye at t = 0 and at equilibrium, V is the solution volume (L) and W is the weight of BC (g). The reaction rate equations according to the isotherm models are presented in Table 2.

Table 2. Isotherm model and equations

Isotherm model	Linear equation	Linear graphs	Constant
Langmuir	$\frac{C_e}{q_e} = \frac{1}{b q_{max}} + \frac{C_e}{q_{max}}$	$\frac{C_e}{q_e}\ vs\ C_e$	$q_{max}\ and\ b$
Freundlich	$log q_e = log K_f + \frac{1}{n} log C_e$	$log q_e\ vs\ log C_e$	$K_f\ and\ n$

q_{max} is the maximum adsorption capacity (mg.g^{-1}).

The q_{max} indicates the maximum MB adsorption capacity (mg.g^{-1}), this value can be calculated from the slope of the Langmuir linear equation.

3. Results and discussions

3.1. Characterization of modified biochar

The FTIR analysis result of modified BCs corresponding to different activation conditions is demonstrated in Fig. 1.

It can be seen that BC has a wide band at 3500-3300 cm^{-1} which is assigned to the O-H stretching mode of the hydroxyl groups. Weak, poorly resolved aliphatic C-H stretching bands between 2750 and 2950 cm^{-1} were also present in the spectra, which is consistent with the expected trends based on prior NMR and FT-IR biochar characterization studies (Kloss et al., 2012; McBeath and Smernik, 2009). The adsorption band at 1650 cm^{-1} is assigned to C=O and C=N stretching. The most intense bands are observed at 1050 cm^{-1}, which is assigned to C-N, C-O stretching of BC. The sharp bands at 461 cm^{-1} were attributed to the presence of Si-O stretching (Lin and Wang, 2014). Therefore, different activation conditions do not affect the bonding of BC.

Raman spectroscopy was used to identify the chemical bonding and intramolecular bonds of the BC with the obtained spectra illustrated in Fig. 2.

The D band was observed at the peak of 1361 cm^{-1}, while the G band was detected at 1591 cm^{-1}. Both were consistent with the sp^2 double-bonded C structure (Amen et al., 2020; Zhang et al., 2018). The overlapping of the bands indicated the amorphous carbon structure, highly corresponding to aromatic carbon, precisely benzene (Ferrari and Robertson, 2000). Considering the similarity of the three spectra, even though the BC went

through different activation conditions, the structure of the materials after pyrolysis remained the same.

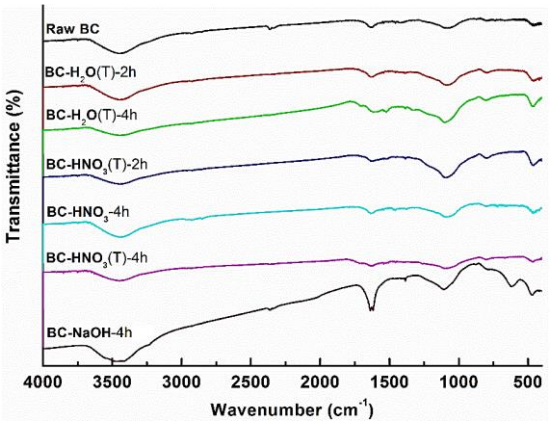

Figure 1. FT-IR diagram of activated biochars

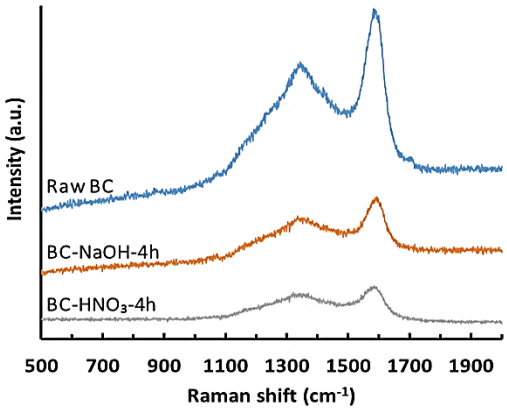

Figure 2. Raman diagram of activated BCs

The diffraction diagram of the BC activated by NaOH-4h in the previous study (Le et al., 2021) showed two wide peaks within a range of 2θ = 22.5° and 2θ = 43° which indicates that the BCs were amorphous carbon. In addition, the diagrams revealed the presence of graphene structure in all BC samples derived from agricultural by-products. This result is similar to the conclusions of BC diffraction studies from Zhang et al. (2012). The activation conditions also do not affect the phase structure of BCs.

PZC values of activated BC are determined by the change of solution pH before and after shaking BC in NaCl solution for 24 hours, as shown in Fig. 3.

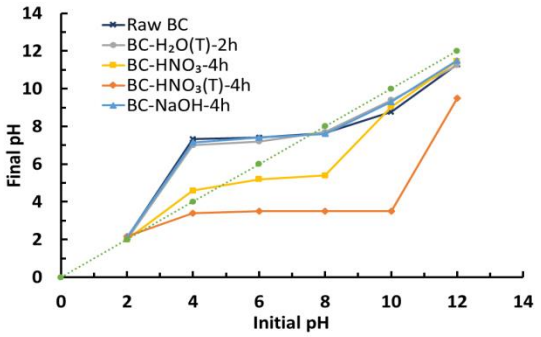

Figure 3. PZC of activated BC derived from rice husk

Figure 3 confirmed that the PZC of raw BC, activated by distilled water, and BC activated by NaOH was equal to 7.8, similar to the results of Adam, (2016) where the pH value of the aqueous solution at room temperature was adjusted to 7.8. However, the values for BC activated by HNO_3 in 4 hours were lower, which is 2 for BC activated at a high temperature and 5 for BC activated at room temperature. Overall, pH 12 might be the best pH for cation removal; however, pH 12 and neutral pH values were chosen for further investigation.

3.2. The adsorption capacity of the activated biochar at different pH

3.2.1. At pH = 12

MB adsorption on activated BC under different conditions was illustrated in Fig. 4.

In general, the adsorption capacity of all materials increased gradually with time and after 6 hours of the experiment. MB adsorption efficiency on activated BC under different conditions increased rapidly in the first hour. When comparing the three different activation agents (water, base, and acid), the results showed that BC activated with NaOH had the highest adsorption capacity compared to the others. The efficiency of this BC rapidly reached equilibrium after 1 hour of

adsorption; following that, BC activated with HNO_3 and with H_2O in last place. In addition, the activity of BC after activation was higher than that of raw BC when adsorbing MB at pH = 12.

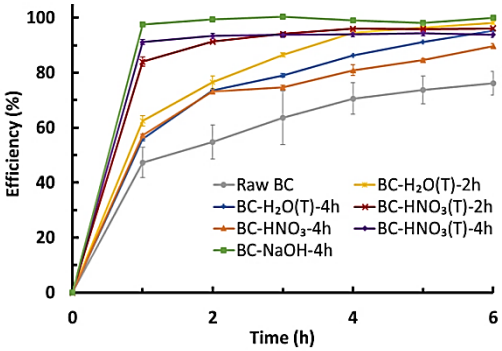

Figure 4. MB adsorption on BC activated under six different conditions and raw BC at pH 12

In terms of temperature, four types of BC activated at high temperature gave higher efficiency than those activated at room temperature, revealing that the activation temperature influences the adsorption capacity of the materials (Ahiduzzaman and Sadrul Islam, 2016; Yang et al., 2019). Uniquely, NaOH was superior, with the highest efficiency, even without being activated at high temperatures. In this study, BC was only activated by NaOH at room temperature because NaOH is corrosive to glass at high temperatures, leading to the possibility of damage to the tools, and if the activation took place in a plastic bottle, there was also a risk of denaturing the plastic.

With the variation of time, the activation of HNO_3 under the same temperature conditions confirmed that the activation time is a negligible effect on the adsorption efficiency of BC. However, when considering activated BC with H_2O, 2 hours of activation was more effective than 4 hours, but the difference was insignificant. This suggests that the activation duration could potentially affect the adsorption efficiency of the material, yet further investigation of this factor is necessary.

Overall, all three factors including activation agent, temperature, and time were proven to impact the adsorption capacity of MB onto BC.

3.2.2. At neutral pH

From the obtained results in Fig. 4 for pH = 12, BC activated with NaOH and with HNO_3 (at high and room temperature) were selected to investigate the removal of MB under neutral pH conditions as in Fig. 5.

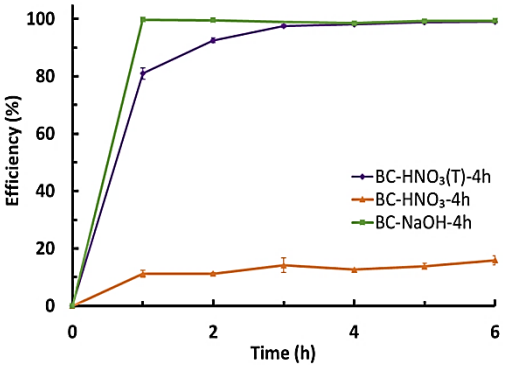

Figure 5. MB adsorption on BC was activated under three different conditions at neutral pH

The MB adsorption efficiency of the material at neutral pH for the same duration of 4 hours tends to increase similar to that at pH = 12, except for the BC activated by HNO_3 at room temperature. NaOH-activated BC's removal efficiency was superior to the others and reached 100% after the first hour, while HNO_3 activated BC at room temperature was just over 10%. The difference could be explained based on the PZC value of each type. As for the PZC of BC activated by HNO_3 (PZC = 5), was much lower than neutral pH, while the PZC of the others was higher than neutral pH. With pH values above their PZC, the adsorbent will adsorb the cations on the MB molecules. Hence the efficiency of the HNO_3 activated

BC at higher temperatures was higher because the lower the pH compared to their PZC value the more negatively charged the adsorbent surface is. With pH value above their PZC, the adsorbent would adsorb the cations on the MB molecules. However, with the pH value below the PZC value, in the case of NaOH (PZC = 8), the removal efficiency of NaOH activated BC was still prominent and reached 100% after the first hour, while HNO_3 activated BC at room temperature was just over 10%. This created a conflict because the MB removal efficiency of BC activated by NaOH should have been lower than the other materials due to the positively charged surface of the adsorbent.

Considering HNO_3, it can be seen that the activation temperature has a strong influence on the ability to remove MB of the material. The higher the activation temperature, the higher the adsorption efficiency is in comparison to BC activated at room temperature.

According to the graphs of Fig. 5, the dye removal efficiency of NaOH activated BC under all reaction conditions constantly gave the best results, reaching the maximum efficiency after only 1 hour of reaction, and the results remained stable in the subsequent measurements. For this reason, BC activated by NaOH was applied in the following experiments. This conclusion also correlated with the research of Youssef et al., (2012). The adsorption of MB onto rice husk activated by NaOH yielded the highest capacity compared to the other conditions due to its highest pore volumes and surface area.

Overall, the pH of the solution significantly affects the adsorption capacity of the material. Different pH values gave various adsorption capacities of the adsorbent. In contrast, at the same pH conditions, the impact of the activation agent, temperature, and time all influenced the efficiency of the adsorbent. The adsorption capacity is closely dependent on the activation methods.

3.3. Adsorption kinetics and isotherms

The adsorption kinetics data of MB adsorption on BC activated with NaOH (10 $mg.L^{-1}$ MB and 5 $g.L^{-1}$ adsorbent) were presented in Figs. 6a-c. The suitability of models depends on the error level-correlation coefficient (R^2) (Kajjumba et al., 2018).

As can be seen, both first- and second-order kinetic models gave a relatively high correlation coefficient, R^2 = 0.9838 and 0.9594, respectively. In addition, the adsorption capacities $q_{e,cal}$ of the first- and second-order kinetic models were nearly equal, 1.7967 $mg.g^{-1}$ and 1.8253 $mg.g^{-1}$ (Table 3), respectively, which were both smaller than $q_{e,exp}$ (2.1725 $mg.g^{-1}$). The experiment for the diffusion model illustrated a linear trend line, with a high R^2 value of 0.9932. However, the line did not pass through the origin, suggesting that the adsorption of MB onto BC was involved in intra-particle diffusion and was not the only rate-controlled step. This process was complex and might involve more than one mechanism (Tiwari et al., 2015).

Overall, the kinetics of MB adsorption onto BC was best described by the linear form of the first-order kinetic model. The adsorption process for the adsorbent was complex with intra-particle diffusion and other rate-controlled steps.

Table 3. Kinetic model parameters

Material	Pseudo first-order			Pseudo second-order		
	q_e ($mg.g^{-1}$)	K_1 (min^{-1})	R^2	K_2 ($g.mg^{-1}.min^{-1}$)	R^2	q_e ($mg.g^{-1}$)
BC	1.7967	0.0032	0.9838	0.0076	0.9594	1.8253

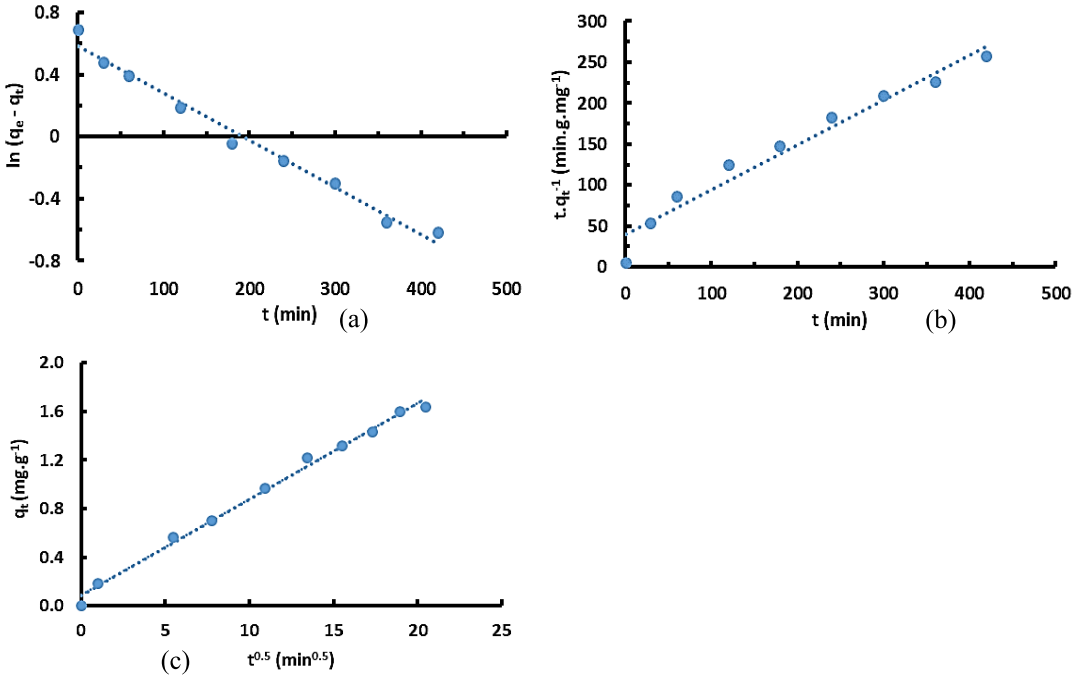

Figure 6. Graph showing the kinetic models for BC - linear pseudo first-order (a), pseudo second-order (b), and intraparticle diffusion (c)

The graphs (Fig. 7) and the data of the Langmuir and Freundlich isotherm models (Table 4) revealed that the Langmuir was the best fit model for BC when adsorbing MB with a high correlation coefficient R^2. In contrast, the Freundlich model gave a much lower output. This finding is consistent with the results of the first-order kinetic model in the adsorption kinetics study above.

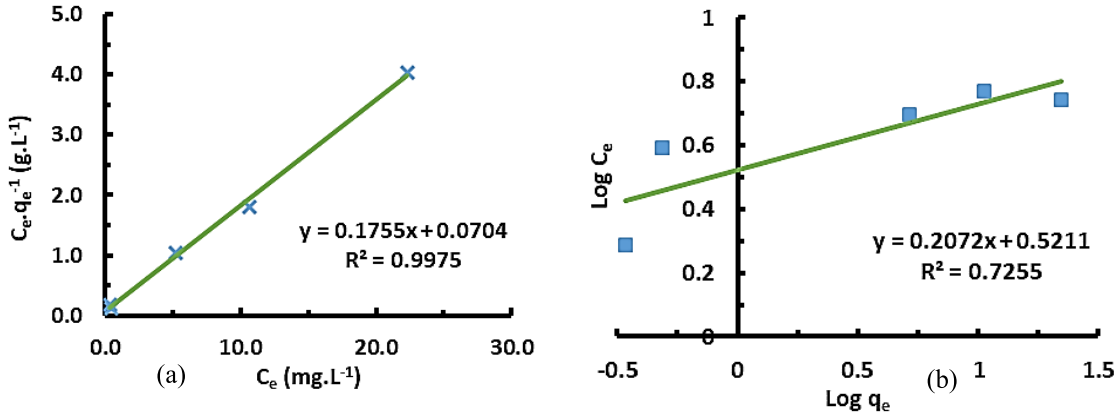

Figure 7. The isotherm models for BC - Langmuir (a) and Freundlich (b)

Table 4. Isotherm model parameters

Material	Langmuir			Freundlich		
	R^2	q_{max} (mg.g^{-1})	B (L.mg^{-1})	R^2	K_f [(mg.g^{-1})(L.mg^{-1})]^n	$1.n^{-1}$
BC	0.9975	5.6980	2.4930	0.7255	3.3200	0.2072

Continuing with the results from Youssef et al. (2012), with the same activation reagent of NaOH, the adsorption of MB onto BC in this research also strictly followed the Langmuir model, whereas, for the adsorption kinetics, it was consistent with the pseudo-second-order with high correlation coefficients for both models compared to the pseudo-first-order of this investigation. This might be due to the difference in the activation method. The rice husk of Youssef et al. (2012) went through a complex multiple-step activation course at high temperatures compared to the simple technique at room temperature in this study. Many papers with different rice husk modification conditions for the adsorption of MB also gave the same results as the Langmuir (Sharma et al., 2010; You et al., 2021) and the second-order adsorption model for MB (Ahmad et al., 2020; Chen et al., 2019; Nworie et al., 2019). Namely, Shih (2012) with different BC modifications of HNO_3, HCl, and H_2SO_4 and the research of Ahiduzzaman and Sadrul Islam (2016) using $ZnCl_2$ activation agent for silica rice husk. In contrast, according to Quansah et al. (2020), in their study of nascent rice husk BC, the pseudo-first-order was aligned with the results of an adsorption capacity of 24.48 $mg.g^{-1}$ at 75°C, which was considered the optimal activation temperature.

Commercial coal was utilized in this study to prevent BC ash formation in the pyrolysis process, where the temperature reached up to 600°C. This solution was more economical than the previous studies of MB adsorption onto BC, where an environment of N_2 gas had to be maintained during the pyrolysis reaction of the rice husk (Ahmad et al., 2020; Nworie et al., 2019; Wang and Liu, 2017).

The inconsistency in the findings with various modifications gives an urge to improve the method of material preparation and further study its principles to optimize the efficiency of BC derived from rice husk when adsorbing MB as well as focus on the reuse of the material to enhance the practical application of rice husk biochar.

4. Conclusions

Rice husk biochar (BC) was derived from local by-product resources as an affordable adsorbent material to treat methylene blue (MB) in wastewater. FTIR, Raman, and PZC were applied to analyze the characterization of BC. After evaluating BC activation conditions, BC activated by NaOH 25% for 4 hours at room temperature was the optimum condition. The dye removal efficiency quickly reached 100% after the first hour in all experiments. The study of activation methods also proved a strong influence of pH, activation agent, temperature, and time upon the MB adsorption capacity of BC. The adsorption kinetics data revealed that the pseudo-first-order kinetic model fit the adsorption of BC, corresponding to the Langmuir isotherm model. Overall, the research showed positive results for the high capability of the BC in terms of textile wastewater treatment, and further studies are necessary to improve the possibilities of the materials.

Acknowledgments

This research was funded by the Vietnam Academy of Science and Technology (VAST), code: VAST07.04/20-21. The authors wish to thank the support of the Land-Ocean aTmosphere regional coUpled System (LOTUS) International Joint Laboratory and the French National Research Institute for Sustainable Development (IRD).

The authors greatly appreciate the editorial team and reviewers who have dedicated their considerable time and expertise to improving the quality of this publication.

Reference

Acemioğlu B., 2019. Removal of a reactive dye using NaOH-activated biochar prepared from peanut shell by pyrolysis process. International Journal of Coal Preparation and Utilization, 0, 1-23. https://doi.org/10.1080/19392699.2019.1644326.

Adam O., 2016. Removal of Resorcinol from Aqueous Solution by Activated Carbon: Isotherms, Thermodynamics and Kinetics. American Chemical Science Journal, 16, 1-13. https://doi.org/10.9734/ACSJ/2016/27637.

Ahiduzzaman Md., Sadrul Islam A.K.M., 2016. Preparation of porous bio-char and activated carbon from rice husk by leaching ash and chemical activation. SpringerPlus, 5, 1248. https://doi.org/10.1186/s40064-016-2932-8.

Ahmad A., Khan N., Giri B.S., Chowdhary P., Chaturvedi P., 2020. Removal of methylene blue dye using rice husk, cow dung and sludge biochar: Characterization, application, and kinetic studies. Bioresource Technology, 306, 123202. https://doi.org/10.1016/j.biortech.2020.123202.

Al-Mamun M.R., Kader S., Islam M.S., Khan M.Z.H., 2019. Photocatalytic activity improvement and application of UV-TiO_2 photocatalysis in textile wastewater treatment: A review. Journal of Environmental Chemical Engineering, 7, 103248. https://doi.org/10.1016/j.jece.2019.103248.

Amen R., Yaseen M., Mukhtar A., Klemeš J.J., Saqib S., Ullah S., Al-Sehemi A.G., Rafiq S., Babar M., Fatt C.L., Ibrahim M., Asif S., Qureshi K.S., Akbar M.M., Bokhari A., 2020. Lead and cadmium removal from wastewater using eco-friendly biochar adsorbent derived from rice husk, wheat straw, and corncob. Cleaner Engineering and Technology, 1, 100006. https://doi.org/10.1016/j.clet.2020.100006.

Bisschops I., Spanjers H., 2003. Literature review on textile wastewater characterisation. Environmental Technology, 24, 1399-1411. https://doi.org/10.1080/09593330309385684.

Chen S., Qin C., Wang T., Chen F., Li X., Hou H., Zhou M., 2019. Study on the adsorption of dyestuffs with different properties by sludge-rice husk biochar: Adsorption capacity, isotherm, kinetic, thermodynamics and mechanism. Journal of Molecular Liquids, 285, 62-74. https://doi.org/10.1016/j.molliq.2019.04.035.

Dargo H., Gabbiye N., Ayalew A., 2014. Removal of Methylene Blue Dye from Textile Wastewater using Activated Carbon Prepared from Rice Husk. International Journal of Innovation and Scientific Research, 9, 317-325.

Desore A., Narula S.A., 2018. An overview on corporate response towards sustainability issues in textile industry. Environment, Development and Sustainability, 20, 1439-1459. https://doi.org/10.1007/s10668-017-9949-1.

Ferrari A.C., Robertson J., 2000. Interpretation of Raman spectra of disordered and amorphous carbon. Physical Review B, 61, 14095-14107. https://doi.org/10.1103/PhysRevB.61.14095

Freundlich, H.M.F., 1906. Over the Adsorption in Solution. The Journal of Physical Chemistry, 57, 385-471.

Hameed B.H., 2008. Equilibrium and kinetic studies of methyl violet sorption by agricultural waste. Journal of Hazardous Materials, 154, 204-212. https://doi.org/10.1016/j.jhazmat.2007.10.010.

Ho Y.S., McKay G., 1999. Pseudo-second order model for sorption processes. Process Biochemistry, 34, 451-465. https://doi.org/10.1016/S0032-9592(98)00112-5.

Holkar C.R., Jadhav A.J., Pinjari D.V., Mahamuni N.M., Pandit A.B., 2016. A critical review on textile wastewater treatments: Possible approaches. Journal of Environmental Management, 182, 351-366. https://doi.org/10.1016/j.jenvman.2016.07.090

Kajjumba G.W., Emik S., Öngen A., Aydın H.K.Ö., S., 2018. Modelling of Adsorption Kinetic Processes Errors, Theory and Application, Advanced Sorption Process Applications. IntechOpen. https://doi.org/10.5772/intechopen.80495.

Kloss S., Zehetner F., Dellantonio A., Hamid R., Ottner F., Liedtke V., Schwanninger M., Gerzabek M.H., Soja G., 2012. Characterization of Slow Pyrolysis Biochars: Effects of Feedstocks and Pyrolysis Temperature on Biochar Properties. Journal of Environmental Quality, 41, 990-1000. https://doi.org/10.2134/jeq2011.0070.

Kuang Y., Zhang X., Zhou S., 2020. Adsorption of Methylene Blue in Water onto Activated Carbon by Surfactant Modification. Water, 12, 587. https://doi.org/10.3390/w12020587.

Kyi P.P., Quansah J.O., Lee C.-G., Moon J.-K., Park S.-J., 2020. The Removal of Crystal Violet from Textile Wastewater Using Palm Kernel Shell-Derived Biochar. Applied Sciences, 10, 2251. https://doi.org/10.3390/app10072251.

Lagergreen S., Svenska B., 1907. Zur Theorie der sogenannten Adsorption gelöster Stoffe. Zeitschrift für Chemie und Industrie der Kolloide, 2, 15-15. https://doi.org/10.1007/BF01501332.

Langmuir, I., 1916. The constitution and fundamental properties of solids and liquids. Journal of the American Chemical Society, 38, 2221-2295. https://doi.org/10.1021/ja02268a002.

Laqbaqbi M., García-Payo M.C., Khayet M., El Kharraz J., Chaouch M., 2019. Application of direct contact membrane distillation for textile wastewater treatment and fouling study. Separation and Purification Technology, 209, 815-825. https://doi.org/10.1016/j.seppur.2018.09.031.

Le P.T., Bui H.T., Le D.N., Nguyen T.H., Pham L.A., Nguyen H.N., Nguyen Q.S., Nguyen T.P., Bich N.T., Duong T.T., Herrmann M., Ouillon S., Le T.P.Q., 2021. Preparation and Characterization of Biochar Derived from Agricultural By-Products for Dye Removal. Adsorption Science Technology, 2021, e9161904. https://doi.org/10.1155/2021/9161904.

Lin J.-Y., Wang B.-X., 2014. Room-Temperature Voltage Stressing Effects on Resistive Switching of Conductive-Bridging RAM Cells with Cu-Doped SiO_2 Films. Advances in Materials Science and Engineering, 2014, e594516. https://doi.org/10.1155/2014/594516

Lin L., Zhai S.-R., Xiao Z.-Y., Song Y., An Q.-D., Song X.-W., 2013. Dye adsorption of mesoporous activated carbons produced from NaOH-pretreated rice husks. Bioresource Technology, 136, 437-443. https://doi.org/10.1016/j.biortech.2013.03.048.

Lin S.H., Peng C.F., 1994. Treatment of textile wastewater by electrochemical method. Water Research, 28, 277-282. https://doi.org/10.1016/0043-1354(94)90264-X.

Manzoor D., Sharma M., 2020. Impact of Textile Dyes on Human Health and Environment, 162-169. https://doi.org/10.4018/978-1-7998-0311-9.ch008.

McBeath A.V., Smernik R.J., 2009. Variation in the degree of aromatic condensation of chars. Organic Geochemistry, 40, 1161-1168. https://doi.org/10.1016/j.orggeochem.2009.09.006.

Nworie F.S., Nwabue F.I., Oti W., Mbam E., Nwali B.U., Nworie F.S., Nwabue F.I., Oti W., Mbam E., Nwali B.U., 2019. Removal of methylene blue from aqueous solution using activated rice husk biochar: adsorption isotherms, kinetics and error analysis. Journal of the Chilean Chemical Society, 64, 4365-4376. https://doi.org/10.4067/s0717-97072019000104365.

Paździor K., Bilińska L., Ledakowicz S., 2019. A review of the existing and emerging technologies in the combination of AOPs and biological processes in industrial textile wastewater treatment. Chemical Engineering Journal, Emerging advanced oxidation technologies and developing perspectives for water and wastewater treatment, 376, 120597. https://doi.org/10.1016/j.cej.2018.12.057.

Qiu H., Lv L., Pan B., Zhang Qing-jian, Zhang W., Zhang Quan-xing, 2009. Critical review in adsorption kinetic models. The Journal of Zhejiang University Science A, 10, 716-724. https://doi.org/10.1631/jzus.A0820524.

Quansah J.O., Hlaing T., Lyonga F.N., Kyi P.P., Hong S.-H., Lee C.-G., Park S.-J., 2020. Nascent Rice Husk as an Adsorbent for Removing Cationic Dyes from Textile Wastewater. Applied Sciences, 10, 3437. https://doi.org/10.3390/app10103437.

Raymundo A.S., Zanarotto R., Belisário M., Pereira M. de G., Ribeiro J.N., Ribeiro A.V.F.N., 2010. Evaluation of sugar-cane bagasse as bioadsorbent in the textile wastewater treatment contaminated with carcinogenic congo red dye. The Brazilian Archives of Biology and Technology, 53, 931-938. https://doi.org/10.1590/S1516-89132010000400023.

Robati D., 2013. Pseudo-second-order kinetic equations for modeling adsorption systems for removal of lead ions using multi-walled carbon nanotube. Journal of Nanostructure in Chemistry, 3, 55. https://doi.org/10.1186/2193-8865-3-55.

Rubeena K.K., Hari Prasad Reddy P., Laiju A.R., Nidheesh P.V., 2018. Iron impregnated biochars as heterogeneous Fenton catalyst for the degradation of acid red 1 dye. Journal of Environmental Management, 226, 320-328. https://doi.org/10.1016/j.jenvman.2018.08.055.

Sala M., Gutiérrez-Bouzán M.C., 2012. Electrochemical Techniques in Textile Processes and Wastewater Treatment. International Journal of Photoenergy, 2012, e629103. https://doi.org/10.1155/2012/629103.

Sarayu K., Sandhya S., 2012. Current Technologies for Biological Treatment of Textile Wastewater - A Review. Applied Biochemistry and Biotechnology, 167, 645-661. https://doi.org/10.1007/s12010-012-9716-6.

Sharma P., Kaur R., Baskar C., Chung W.-J., 2010. Removal of methylene blue from aqueous waste using rice husk and rice husk ash. Desalination, 259, 249-257. https://doi.org/10.1016/j.desal.2010.03.044.

Shih M.-C., 2012. Kinetics of the batch adsorption of methylene blue from aqueous solutions onto rice husk: effect of acid-modified process and dye concentration. Desalination and Water Treatment, 37, 200-214. https://doi.org/10.1080/19443994.2012.661273.

Shoukat R., Khan S.J., Jamal Y., 2019. Hybrid anaerobic-aerobic biological treatment for real textile wastewater. Journal of Water Process Engineering, 29, 100804. https://doi.org/10.1016/j.jwpe.2019.100804

Siddique K., Rizwan M., Shahid M.J., Ali S., Ahmad R., Rizvi H., 2017. Textile Wastewater Treatment Options: A Critical Review, in: Anjum N.A., Gill S.S., Tuteja N. (Eds.), Enhancing Cleanup of Environmental Pollutants: 2: Non-Biological Approaches. Springer International Publishing, Cham, 183-207. https://doi.org/10.1007/978-3-319-55423-5_6.

Tiwari M., Shukla S., Kisku G., 2015. Linear and Non-Linear Kinetic Modeling for Adsorption of Disperse Dye in Batch Process. Research Journal of Environmental Toxicology, 9. https://doi.org/10.3923/rjet.2015.320.331.

Wang M., Wang J.J., Wang X., 2018. Effect of KOH-enhanced biochar on increasing soil plant-available silicon. Geoderma, 321, 22-31. https://doi.org/10.1016/j.geoderma.2018.02.001.

Wang Y., Liu R., 2017. Comparison of characteristics of twenty-one types of biochar and their ability to remove multi-heavy metals and methylene blue in solution. Fuel Processing Technology, 160, 55-63. https://doi.org/10.1016/j.fuproc.2017.02.019.

Weber W.J., Morris J.C., 1963. Kinetics of Adsorption on Carbon from Solution. Journal of the Sanitary Engineering Division, 89, 31-60.

Yang X., Zhang S., Ju M., Liu L., 2019. Preparation and Modification of Biochar Materials and their Application in Soil Remediation. Applied Sciences, 9, 1365. https://doi.org/10.3390/app9071365.

You X., Wang R., Zhu Y., Sui W., Cheng D., 2021. Comparison of adsorption properties of a cellulose-rich modified rice husk for the removal of methylene blue and aluminum (III) from their aqueous solution. Industrial Crops and Products, 170, 113687. https://doi.org/10.1016/j.indcrop.2021.113687.

Youssef A.M., Ahmed A.I., El-Bana U.A., 2012. Adsorption of cationic dye (MB) and anionic dye (AG 25) by physically and chemically activated carbons developed from rice husk. Carbon Letters, 13, 61-72. https://doi.org/10.5714/CL.2012.13.2.061

Zazycki M.A., Godinho M., Perondi D., Foletto E.L., Collazzo G.C., Dotto G.L., 2018. New biochar from pecan nutshells as an alternative adsorbent for removing reactive red 141 from aqueous solutions. Journal of Cleaner Production, 171, 57-65. https://doi.org/10.1016/j.jclepro.2017.10.007

Zhang K., Sun P., Faye M.C.A.S., Zhang Y., 2018. Characterization of biochar derived from rice husks and its potential in chlorobenzene degradation. Carbon, 130, 730-740.

https://doi.org/10.1016/j.carbon.2018.01.036

Zhang M., Gao B., Yao Y., Xue Y., Inyang M., 2012. Synthesis, characterization, and environmental implications of graphene-coated biochar. Science of The Total Environment, 435-436, 567-572. https://doi.org/10.1016/j.scitotenv.2012.07.038.

Zhao L., Zheng W., Mašek O., Chen X., Gu B., Sharma B.K., Cao X., 2017. Roles of Phosphoric Acid in Biochar Formation: Synchronously Improving Carbon Retention and Sorption Capacity. Journal of Environmental Quality, 46, 393-401. https://doi.org/10.2134/jeq2016.09.0344.